



HAL
open science

Multi-Objective Ensemble-Processing Strategies to Optimize the Simulation of the Western North Pacific Subtropical High in Boreal Summer

Cenxiao Sun, Zhihong Jiang, Zhenfei Tang, Laurent Li

► **To cite this version:**

Cenxiao Sun, Zhihong Jiang, Zhenfei Tang, Laurent Li. Multi-Objective Ensemble-Processing Strategies to Optimize the Simulation of the Western North Pacific Subtropical High in Boreal Summer. *Geophysical Research Letters*, 2023, 50 (23), pp.e2023GL107040. 10.1029/2023GL107040. hal-04322318

HAL Id: hal-04322318

<https://hal.science/hal-04322318>

Submitted on 4 Dec 2023

HAL is a multi-disciplinary open access archive for the deposit and dissemination of scientific research documents, whether they are published or not. The documents may come from teaching and research institutions in France or abroad, or from public or private research centers.

L'archive ouverte pluridisciplinaire **HAL**, est destinée au dépôt et à la diffusion de documents scientifiques de niveau recherche, publiés ou non, émanant des établissements d'enseignement et de recherche français ou étrangers, des laboratoires publics ou privés.

Geophysical Research Letters[®]



RESEARCH LETTER

10.1029/2023GL107040

Key Points:

- Sea surface temperatures from three key basins are used to constrain the simulation of the western North Pacific Subtropical High
- The performance of models' ensemble can be improved when implementing physical links in processing multi-model ensemble simulations
- Spurious states of the Pareto-optimal scheme can be eliminated with additional conditions of least errors

Supporting Information:

Supporting Information may be found in the online version of this article.

Correspondence to:

Z. Jiang,
zhjiang@nuist.edu.cn

Citation:

Sun, C., Jiang, Z., Tang, Z., & Li, L. (2023). Multi-objective ensemble-processing strategies to optimize the simulation of the western North Pacific Subtropical High in boreal summer. *Geophysical Research Letters*, 50, e2023GL107040. <https://doi.org/10.1029/2023GL107040>

Received 27 OCT 2023
Accepted 13 NOV 2023

Author Contributions:

Conceptualization: Zhihong Jiang, Laurent Li
Data curation: Cenxiao Sun
Formal analysis: Cenxiao Sun, Zhihong Jiang
Funding acquisition: Zhihong Jiang
Software: Cenxiao Sun, Zhenfei Tang
Writing – original draft: Cenxiao Sun, Zhihong Jiang
Writing – review & editing: Cenxiao Sun, Zhihong Jiang, Laurent Li

© 2023. The Authors.

This is an open access article under the terms of the [Creative Commons Attribution-NonCommercial-NoDerivs License](https://creativecommons.org/licenses/by-nc-nd/4.0/), which permits use and distribution in any medium, provided the original work is properly cited, the use is non-commercial and no modifications or adaptations are made.

Multi-Objective Ensemble-Processing Strategies to Optimize the Simulation of the Western North Pacific Subtropical High in Boreal Summer

Cenxiao Sun¹, Zhihong Jiang¹ , Zhenfei Tang^{1,2}, and Laurent Li³ 

¹Key Laboratory of Meteorological Disaster of Ministry of Education (KLME), Collaborative Innovation Center on Forecast and Evaluation of Meteorological Disaster, Nanjing University of Information Science and Technology, Nanjing, China, ²Fujian Climate Center, Fujian Province Meteorology Bureau, Fuzhou, China, ³Laboratoire de Météorologie Dynamique, IPSL, CNRS, Sorbonne Université, Ecole Normale Supérieure, Ecole Polytechnique, Paris, France

Abstract The western North Pacific Subtropical High (WNPSH) in boreal summer is a major atmospheric player affecting East Asian climate, but its simulation in state-of-the-art climate models is still largely biased. Here we use a multi-objective optimization strategy, the Pareto optimality, to incorporate multiple physical constraints in processing multi-model simulations provided by the Coupled Model Intercomparison Project Phase 6. We aim to improve the simulation of WNPSH by this practice. Sea surface temperatures from three tropical oceanic basins are found highly related to WNPSH, and thus used as constraints. We also present an ameliorated strategy, which takes a subset of the raw Pareto optimality by imposing conditions of smallest errors. Results show that the overestimate of WNPSH is effectively corrected. The two multi-objective optimization schemes both perform better than the traditional approach, revealing the importance of implementing physically based links in processing multi-model ensemble simulations.

Plain Language Summary The western North Pacific Subtropical High (WNPSH) in boreal summer exerts important impact on East Asian climate, but its simulation in climate models is still largely biased. In order to improve its simulation, we use an optimization strategy involving Pareto-optimality endowed with the ability to take multiple objectives into consideration to constrain climate models. Sea surface temperatures from three tropical oceanic basins are found highly related to the WNPSH, and thus used as constraining co-variables in the optimization. We also present an ameliorated strategy, by imposing additional conditions to further constrain the procedure and ameliorate the results. The two multi-objective optimization schemes are finally compared with a traditional ensemble-processing scheme that uses the same geophysical co-variables but without considering any physical constraints among them. The superiority of the multi-objective optimization is unequivocally demonstrated.

1. Introduction

Known as a key component of the East Asian summer monsoon system, the western North Pacific Subtropical High (WNPSH) exerts tremendous impacts on climate in Eastern China (C. Li et al., 2021; Luo & Lau, 2017; W. Wang et al., 2016; Zhang & Tao, 2003). However, there are still large biases for climate models to simulate WNPSH, creating uncertainties for the simulation of the East Asian summer monsoon (Song & Zhou, 2014; Zhao et al., 2020; Zhou et al., 2018). It is generally believed that the multi-model ensemble mean (or median) can improve the collective performance, since biases of individual models can be offset and canceled out. The collective performance can be even further enhanced if the performance of individual models is used as weight in the ensemble-processing strategy (Jiang et al., 2015; Li, Jiang, Zhao, & Li, 2021; Tan et al., 2016).

It is worthy of note that most ensemble-processing schemes use algorithms focusing on a single performance or cost function. These schemes generally pay less attention to physical processes or constraints relating geophysical variables one to another, which constitutes their weakness (Herger et al., 2019; Langenbrunner & Neelin, 2017b). Actually, feedbacks relating different geophysical variables may play an essential role in the climate system. It would be beneficial if the measuring of model performance is based on such feedbacks or physical processes. In the case of WNPSH, its links to sea surface temperatures (SSTs) should be the most important processes to be taken into account (He, Zhou, & Wu, 2015; Zeng et al., 2010; Zhou et al., 2009). Especially, tropical and subtropical ocean basins are proved to have the largest effects on WNPSH, including the tropical Indian Ocean

(Wu et al., 2009; Xie et al., 2009), the Maritime Continent (Chuang et al., 2011; B. Wang et al., 2000; J. Zhu et al., 2022), the tropical Pacific (B. Wang et al., 2013; Xiang et al., 2013; Ying & Sun, 2000), and the Atlantic (Hong et al., 2014; Zuo et al., 2019).

To improve the performance of physically connected variables in climate models, the concept “Pareto-optimality” provides an interesting tool that can optimize multiple objectives simultaneously. It is a concept first used in economics by Pareto, referring to an ideal state that one cannot gain more benefits or interests without harming others through a reallocation of limited resources (Pareto, 1906). While traditional ensemble-processing schemes have difficulty in reconciling effects among multiple objectives, the Pareto-optimality potentially offers an approach to reach states in which the performance of one climate variable cannot be further improved without degeneration of another.

There are a few works reported in the literature using this general idea. Langenbrunner and Neelin (2017a) used the Pareto-optimality to adjust tunable parameters of climate models. Subsequently, they also used it to constrain the projection of precipitation in California by using the physically related tropical Pacific SST and the 200 hPa zonal winds over the west coast of America, and the uncertainty of precipitation changes in the end of 21st century is decreased by nearly 70% (Langenbrunner & Neelin, 2017b). A similar conclusion of precipitation in California constrained by causal links is also drawn in F. Li et al. (2022) based on this scheme. In Herger et al. (2019) targeting precipitation over Australia, the whole Pacific SST and 500 hPa eastward wind over high latitude in the Southern Ocean were taken as constraining co-variables. They furthermore pointed out that it is important to associate physical explanations for the relationship among co-variables when a multi-objective constraining scheme is used.

As a strategy to treat multi-model ensemble, however, the Pareto optimality has not been assessed against other more traditional strategies using weights deduced from model performance measured with single variable or each of the individual variables. A major limitation of these traditional strategies is certainly related to the fact that they generally can't consider physical links among variables (Jiang et al., 2015; W. Li et al., 2016; Li, Jiang, Zhao, & Li, 2021; Tan et al., 2016), it should be noted that the Pareto-optimal ensemble is also an imperfect one. A Pareto-optimal multi-objective scheme faces inevitable risks in model evaluation. In the case that a climate model, among all others, performs extremely well in the simulation of variable A but quite poorly (though not the worst) in variable B, it may also be chosen as a member of the “Pareto-optimal ensemble.” In this case, the Pareto-optimal scheme tends to excessively rely on model performance of a single variable, meaning that the “optimal ensemble” may not represent models with simultaneously good performance for all geophysical variables.

To explore these issues, by taking the WNPSH as an example, we make use of the traditional statistic algorithm of Rank-based weighting scheme (W. Chen et al., 2011; Jiang et al., 2015) and a newly defined weighting scheme to assess the optimization effect of the Pareto-optimal scheme. This study aims at better understanding these multi-objective optimization schemes and contributing to researches on future climate projection.

2. Data and Methods

2.1. Model and Observation Data

Data used in this study are monthly sea level pressure (SLP) and sea surface temperature (SST) under historical simulations from 22 CMIP6 models (as shown in Table S1 in Supporting Information S1), a single member is taken from each model. Two reanalysis data sets are taken as observations, including monthly SLP from the European Centre for Medium-Range Weather Forecasts (ECMWF) fifth-generation (ERA5) reanalysis with horizontal resolution of $0.25^\circ \times 0.25^\circ$ and the monthly extended $2^\circ \times 2^\circ$ Version 5 reconstructed SST (ERSSTv5) (Hersbach et al., 2020; B. P. Huang et al., 2017). Before analysis, all simulated and reanalyzed data are re-gridded to a common $2.5^\circ \times 2.5^\circ$ grid. This study focuses on June, July, and August due to the fact that strong impacts of WNPSH on East Asian climate are generally in boreal summer.

To reduce the influence from systematic biases of individual CMIP6 models and to amplify the signal of large-scale patterns of SLP and SST, the climatology of zonal mean SLP between 0 and 40°N and areal-mean SST of the tropical Indo-Pacific basin (here 30°S – 30°N , 30°E – 70°W) for the studied period is subtracted in each model and observation before further processing. Such a preprocessing is a common practice, often used in

studies related to WNPSH (X. Chen et al., 2020; He, Zhou, Lin, et al., 2015; Y. Huang et al., 2016). Actually, by doing so, we privilege spatial patterns of both SLP and SST, rather than their absolute levels.

2.2. Ensemble-Processing Methods and Evaluation Metrics

The multi-model ensemble simulations provided by CMIP modelers constitute our basic database. A particularity of the Pareto-optimality is that it doesn't optimize a single synthetic cost function, a common strategy in other multi-model approaches, but explores joint properties of multiple variables. Each variable expresses an objective or a process, and represents a physical constraint. Our Pareto-optimal multi-objective ensemble scheme is adopted from Langenbrunner and Neelin (2017b), based on a Python Package designed by Woodruff and Herman (2014).

In our work, to avoid degeneration of the algorithm, it is necessary to perform the optimization over a large-size ensemble. Similar to Langenbrunner and Neelin (2017b), we generate a sufficient number of combinations from original models by exhaustively combining the 22 CMIP6 models (through arithmetic average) with k (here $1 \leq k \leq 5$) randomly selected members (combination 22 choose k , noted as C_k^{22}). As a result, there are totally $35,442 \left(\sum_{k=1}^5 C_k^{22} \right)$ subsets. It is to be noted that the climatology for both SLP and SST is from a general average in the studied period and across all members of the sub-ensemble. The metrics for bias assessment between model simulations and observations are based on root mean square error (RMSE, applied to climatological spatial fields) of all variables, smaller RMSE representing better model performance.

Though the Pareto-optimal multi-model ensemble-processing scheme has the ability to select a subset of samples, which improve the performance of one variable without degradation in another, it still faces nonnegligible risk. Some members have good simulation skill in one variable but poor skill in another may also be selected. To remediate this issue, we define an alternative method named "Least-distance strategy over Pareto-optimality" (abbreviated as Least-distance strategy) to further constrain the Pareto-optimal samples to avoid such deficiency. The Least-distance strategy is detailed in Text S1 and Figure S1 in Supporting Information S1. The Rank-based weighting method (W. Chen et al., 2011), which doesn't take into account any physical links among geophysical variables, is used for the purpose of inter-comparison with the above two schemes. The weighting method is given in Text S2 in Supporting Information S1.

For the purpose of independent verification, we divide the historical period into the calibration period from 1961 to 1987 and validation period from 1988 to 2014, both covering 27 years. To evaluate the skill of different ensemble-processing methods in reproducing the spatial pattern between the simulation and observation, the Taylor diagram and Taylor skill score (TSS) were used (Li, Jiang, Treut, et al., 2021; Taylor, 2001; H. Zhu et al., 2020), which is described in Text S3 in Supporting Information S1.

3. Results

3.1. Determining Co-Variables to Constrain WNPSH

To avoid the general rising effect of geopotential height under global warming which prevents us from using it as a surrogate of WNPSH, we choose SLP to represent WNPSH as in Preethi et al. (2017) and X. Chen et al. (2020). Furthermore, to enhance the role of large scale SLP patterns, and to reduce the influence of systematic biases of individual CMIP6 models, SLP was first subtracted from its zonal mean between 0° and 40°N . It is clear that this preprocessing preserves the spatial pattern of SLP (Figure S2 in Supporting Information S1). The shading in Figure S2a in Supporting Information S1 indicates the inter-model standard deviation of SLP biases in the whole historical period (1961–2014). Figure S2b in Supporting Information S1 shows the counterpart after the pre-processing. It can be seen that large inter-model spread exists. The largest standard deviation over the north-east Pacific reflects the important dispersion of the center of the North Pacific Subtropical High. Meanwhile, the second center of large dispersion over the northwest Pacific shows large diversity among models for its western extension. Since the western extension of WNPSH is the most important feature for East Asian climate, we thus select this region ($15^\circ\text{--}40^\circ\text{N}$, $120^\circ\text{--}180^\circ\text{E}$, red boxes in Figure S2 in Supporting Information S1) to represent WNPSH.

Previous studies concluded that there are tight physical relationships between SST and WNPSH. For the sake of completeness and objectivity, we can reconfirm their links at interannual scale with a Singular Value Decomposition (SVD) analysis applied to the pre-processed SLP over the Northwest Pacific and SST over the tropical

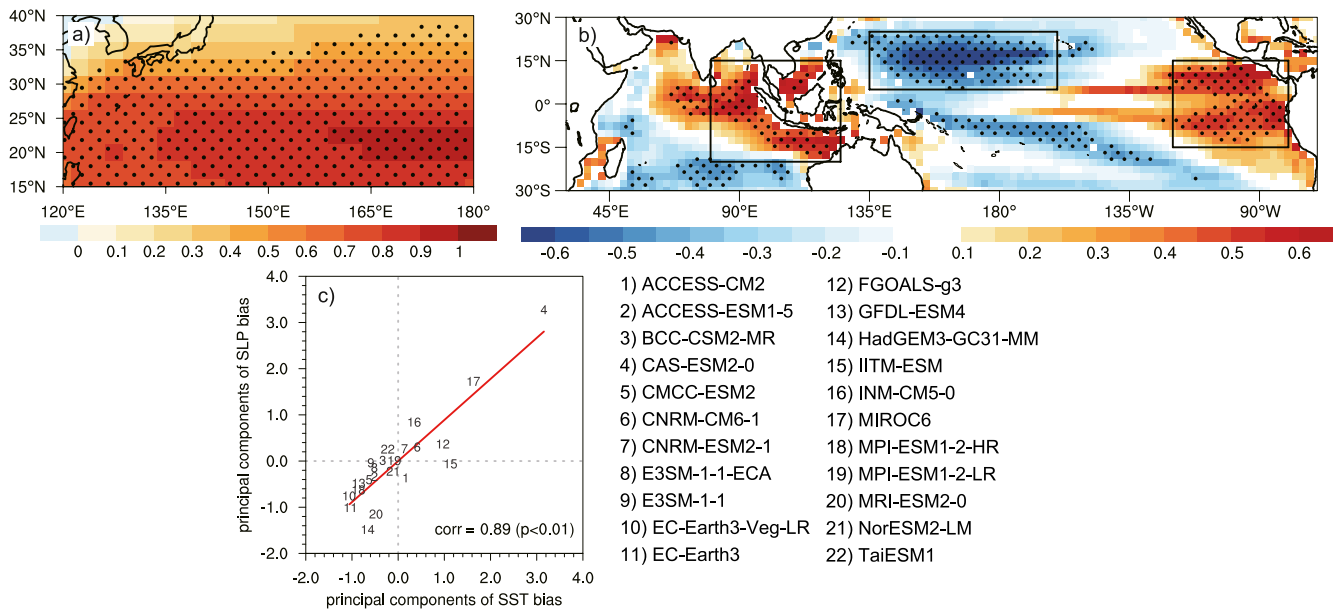


Figure 1. Leading Singular Value Decomposition heterogeneous correlation maps for the standardized inter-model biases of pre-processed sea level pressure (SLP) (a) and tropical Indo-Pacific sea surface temperature (SST) (shading in panel (b)) in the calibration period (1961–1987). Dotted areas represent statistically significant correlations according to a 10% level two-sample *t*-test. The black box in panel (a) outlines the western North Pacific Subtropical High target region, and those in panel (b) represent the key regions of SST as constraining co-variables, including the Maritime Continent (MC: 20°S–15°N, 80–125°E), the tropical central Pacific (CP: 5°–25°N, 135°E–160°W), and eastern Pacific (EP: 15°S–15°N, 80–120°W). (c) The standardized corresponding principal components of CMIP6 models, shown by numbers. The abscissa represents SST and the ordinate SLP, the correlation coefficient and *p*-value are marked at the bottom right. The gray lines in panel (c) show the value of 0 and red line represents the regression.

Indo-Pacific sector, with long-term trend previously removed. Results in the calibration period (1961–1987) are displayed in Figure S3 in Supporting Information S1. The leading SVD (SVD1), which explains 57.7% of the total square covariance, shows a strong SLP center in the western North Pacific (Figure S3a in Supporting Information S1). Areas of significant positive correlation are found over the North Indian Ocean, the Maritime Continent and the tropical eastern Pacific, while significant negative correlation lies over the Central Pacific (Figure S3b in Supporting Information S1). Actually, it is believed that warm SST over the Indian Ocean can affect WNPSH through its capacitor effect (Wu et al., 2009; Xie et al., 2009), and warm anomalies of SST in the Maritime Continent and in the Eastern Pacific can enhance WNPSH through anomalous descending motions, induced by the intensified Hadley circulation (He, Zhou, & Wu, 2015; J. Zhu et al., 2022) and the weakened Walker circulation (Y. Li et al., 2010; Ying & Sun, 2000). Cold SST anomalies in the Central Pacific can furthermore inhibit the local precipitation and convection, leading to intensification of WNPSH (B. Wang et al., 2013; Xiang et al., 2013).

The relationship between SST and SLP at the level of inter-model biases is further explored in order to build the multi-objective constraining scheme, by performing a similar SVD analysis, but applied to the inter-model variability of models' climatological fields in the calibration period. SVD1 is shown in Figure 1, displaying the heterogeneous correlation maps of SLP biases (Figure 1a) and SST biases (Figure 1b). SVD1 accounts for 66.0% of the total square covariance, representing the main relationship between the biases of the two simulated variables. The high correlation in Figure 1a in the Northwest Pacific reveals that the inter-model biases of WNPSH are significantly correlated with SST biases. Two large regions of significant positive correlation appear near the Maritime Continent and Eastern Pacific, meaning that models with overestimated SST here may tend to simulate stronger WNPSH bias. A significant negative correlation is located in the central Pacific (Figure 1b), suggesting that underestimating SST here may also lead to a corresponding overestimated WNPSH. These features in Figure 1 are consistent with what shown in Figure S3 in Supporting Information S1, though their nature is different, revealing that the inter-model relationship in climatological biases of SST and SLP is consistent with the observed interannual variability that is physically generated.

Based on the above discussion of the relationship between SLP and SST in observation and across climate models, we finally choose SST from three key oceanic basins as WNPSH's co-variables in our multi-objective constraining algorithm. They are the Maritime Continent (MC: 20°S–15°N, 80–125°E), the tropical central

Pacific (CP: 5°–25°N, 135°E–160°W) and the tropical eastern Pacific (EP: 15°S–15°N, 80°–120°W), highlighted by the black boxes in Figure 1b.

3.2. Multi-Objective Pareto Optimality Versus Ranking With Multiple Variables

In this section, we quantitatively assess the performance of climate models in reproducing the climatological spatial pattern of SLP and SSTs, with the two multi-objective optimization methods, that is, the Pareto-optimality and the Least-distance strategy. The performance of the traditional statistic algorithm of Rank-based weighting scheme (with multiple variables independently considered) is also presented as a reference to explore the effectiveness and efficiency of the two multi-objective Pareto-optimality schemes, which take into account the physically based links among geophysical variables.

3.2.1. Pareto-Optimal Multi-Model Ensemble-Processing Scheme

The RMSE of the four co-variables (SLP and three SST) is used as the model performance metrics. Smaller RMSE means better performance. The Pareto-optimal algorithm tends to select a subset of samples with smaller RMSE for the four co-variables, satisfying the exigence of improving the performance of one variable without degrading any others. Results are displayed in Figure S4 in Supporting Information S1 in the form of scatter plot. Each axis represents the corresponding co-variable's RMSE. It is clear that the Pareto-optimality operation successfully selected a subset of states, with much smaller RMSE, situated at the edge of the gray-dot cloud. This implies that the Pareto-optimality considers all co-variables and adjust them simultaneously, and the processes linking the co-variables entered into action during the optimization.

For a given Pareto-optimal subset, its composition of CMIP6 models shows a fixed configuration which allows us to deduce models' weight if we only consider the Pareto-optimal ensemble mean. For example, if a Pareto-optimal subset contains five models, a number of 0.2 (1/5) is the number of hits for each of the five models in the ensemble. The same calculation can be applied to a Pareto-optimal ensemble, regardless of its size (1815 here).

3.2.2. Least-Distance Strategy Over Pareto-Optimality

As mentioned in Introduction, there are some risks in the Pareto-optimal multi-model ensemble scheme. To explore this point, we define the least-distance strategy to further constrain the Pareto-optimal subset. A threshold for each co-variable is determined with a percentile criterion for the Pareto-optimal samples. Histograms of these Pareto-optimal samples are shown in Figure S5 in Supporting Information S1, following each of the four axes. To ensure equality of all co-variables, a same percentile (here the 90th one, shown by purple dash lines in Figure S5 in Supporting Information S1) is used to select the four different thresholds. Pareto-optimal sub-samples falling in the 4-dimensional space circled by the selected thresholds can then form a new subset, shown by purple dots in Figure S4 in Supporting Information S1, containing only 150 samples. In terms of model weighting, we can express weights in a same way as practiced for the Pareto-optimal scheme.

3.2.3. Rank-Based Weighting Scheme

To compare with the two multi-objective optimization methods, the traditional statistic algorithm of Rank-based weighting scheme is used. Sorting the RMSE of CMIP6 models for each co-variable and the weights can be obtained from models' rank. It should be noted that though we use four co-variables in the Rank-based weighting method, the process of ranking is independent from each other. No physical links are considered when ranking.

Let us now compare the two multi-objective optimality schemes and the Rank-based scheme in terms of model weighting, as shown in Figure 2, which ranks models from left to right following weights obtained by the Least-distance strategy. It can be seen that the three lines have similar behaviors, showing that they all capture the basic effects of CMIP6 models. Actually, 9 out of the top 10 models and 7 out of the bottom 10 models are common among all ensemble-processing schemes. Due to the additional constraining conditions over Pareto-optimality, the Least-distance strategy shows the largest gradient, indicating that this scheme enhances the effect of well-performed models and weakens the poorly behaved ones to a greater extent. Weights provided by the Rank-based method are the flattest, meaning that it is the least discriminant.

3.3. Performance Evaluation

The evaluation is given in the independent validation period (1988–2014). Taylor diagrams and TSSs are used to assess the overall skills (Figure 3). The performance is improved in all the weighted results compared to the

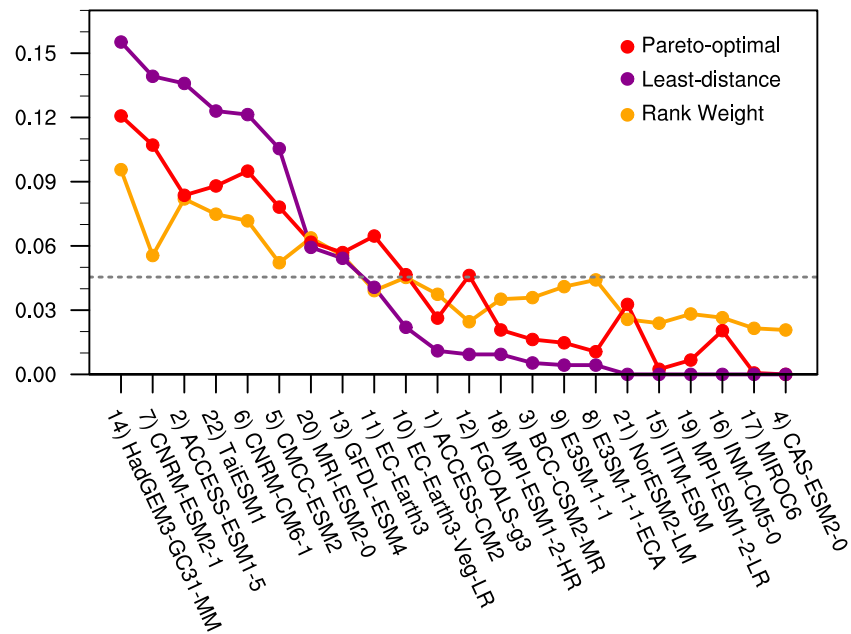


Figure 2. The models' weights obtained by the Pareto-optimal scheme (red dots), Least-distance strategy scheme (purple dots), and Rank-based weighting scheme (yellow dots). The models of x-axis are ordered by weights of Least-distance strategy from the highest weights to the lowest. The dashed line indicates equal-weights for all models (0.045, i.e., 1 divided by the number of models).

simple arithmetic mean (CMIP6-MME). The Pareto-optimal scheme has a good performance, whose correlation coefficient is bigger and the standard deviation ratio is closer to 1, compared to the Rank-based weighting method and CMIP6-MME. TSS is also obviously higher in the Pareto-optimal scheme, with 0.995, 0.990, 0.922, and 0.960 for SLP, MC, CP, and EP-SST, respectively. The Least-distance strategy shows further improvement. All co-variables are closer to the observation in Taylor diagrams, and the TSS is 0.996, 0.989, 0.945, and 0.965 for SLP, MC, CP, and EP-SST, respectively. Though TSS of MC-SST is slightly lower than the counterpart in the Pareto-optimal scheme, the Least-distance strategy, as a whole, can be regarded as the best-performed method. Such a configuration shows clearly that the Least-distance strategy is successful in eliminating the few samples of the Pareto-optimality with relatively large RMSE (although they do lie in the smaller-RMSE part among all samples). As regards the Rank-based weighting method, it shows better performance than CMIP6-MME, but its skill is much behind the Pareto-optimality and the Least-distance strategy.

The spatial patterns of SLP climatology, together with its biases, obtained with the four ensemble-processing schemes are shown in Figure S6 in Supporting Information S1 for the independent validation period. It is not a surprise that all ensemble-processing schemes capture the main features of SLP. However, WNPSH in CMIP6-MME, with a westward extension, is obviously too strong, compared to the observation (shown by green contours in Figure S6 in Supporting Information S1). The spatial distribution of biases clearly reveals such an overestimation (Figure S6e in Supporting Information S1), showing large positive biases over the Northwest Pacific, by more than 1.6 hPa. The weighting schemes improve the result. In Figures S6b–S6d in Supporting Information S1, it can be seen that all of them improve the characteristics of WNPSH, make it closer to the observation. Positive biases over the Northwest Pacific are effectively reduced to a level of 0.7 and 0.4 hPa in the Pareto-optimal and Least-distance strategy schemes, which is a reduction of 56% and 75% relative to CMIP6-MME. However, SLP around 30°N, 130°E is a little underestimated in the two multi-objective optimal schemes, this is because the high-weighted CMIP6 models represent relatively low SLP in this area. The Rank-based weighting scheme also reduces the bias, but only to a level of about 1 hPa (Figure S6h in Supporting Information S1). The RMSE in the studied area (black boxes in Figure S6 in Supporting Information S1) is 0.33/0.32/0.53 hPa in the Pareto-optimal/Least-distance/Rank-based schemes, respectively. That is a reduction of 55/57/28% relative to CMIP6-MME (in which RMSE is 0.74 hPa).

The simulated spatial distribution of the tropical Indo-Pacific SST is displayed in Figure S7 in Supporting Information S1. It is obvious that the bias of SST is also reduced in the Pareto-optimal and Least-distance strategy schemes, compared to the Rank-based scheme (Figure S7 in Supporting Information S1). Overall, the largest

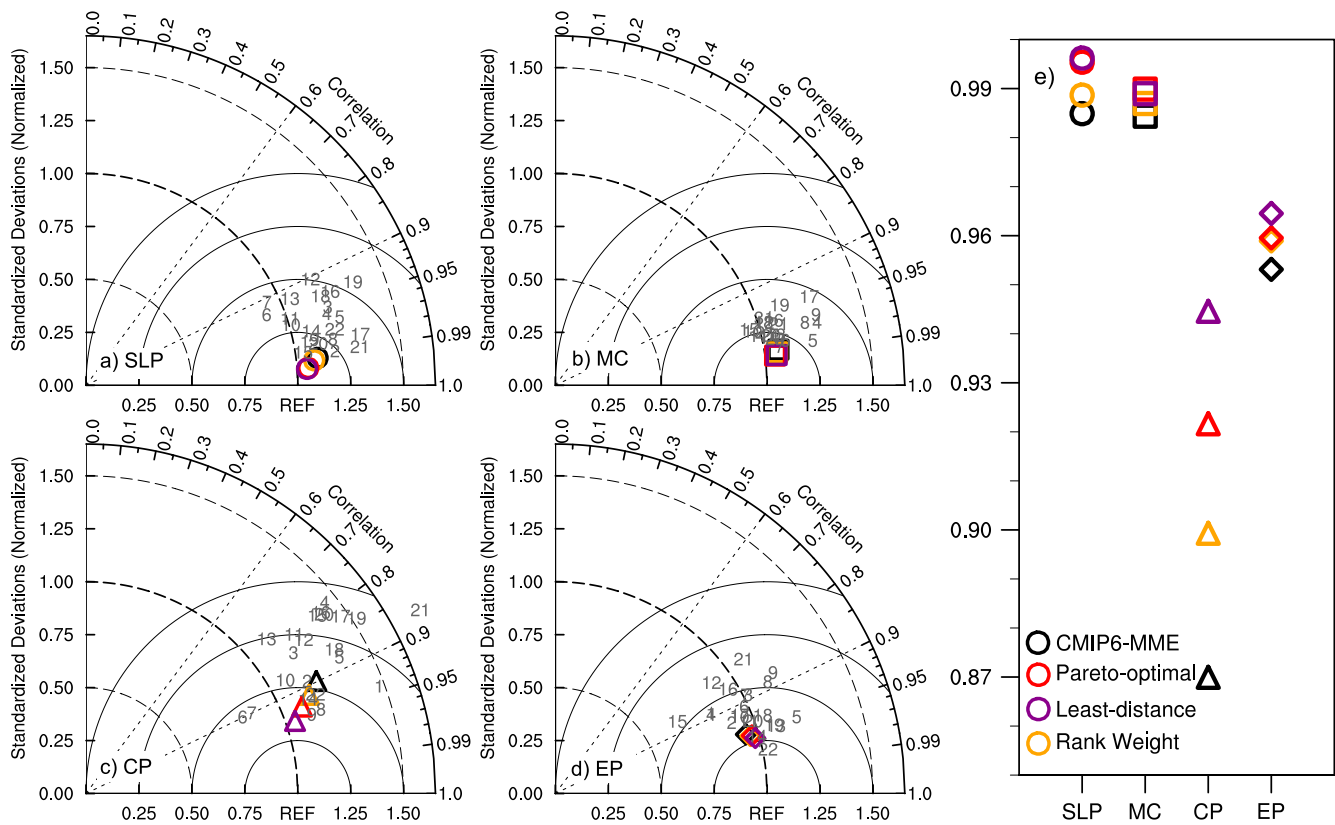


Figure 3. Taylor diagram (a–d) showing the sea level pressure, MC-SST, CP-SST, and EP-SST of individual CMIP6-models (gray numbers) and four ensemble schemes of CMIP6-MME (black symbols), Pareto-optimal scheme (red symbols), Least-distance strategy (purple symbols), and Rank-based weighting scheme (yellow symbols) during the validation period (1988–2014). The number of CMIP6 models are the same as in Figure 1. (e) Taylor skill score of four co-variables simulated by four ensemble schemes. Different colors represent different ensemble scheme, and different symbols represent different co-variables.

improvement occurs in Least-distance strategy, which is consistent with the evaluation shown in Figure 3. These results indicate that, compared to the traditional Rank-based weighting scheme, the multi-objective schemes with physical links considered have stronger ability to improve model performance, and the Least-distance scheme imposes further constraints to the Pareto-optimal subset.

4. Discussion and Conclusion

The approach of ensemble simulations with multiple models is a common effort of the international community to tackle numerous climate issues. It is generally believed that the collective performance can be enhanced through an optimal usage of the ensemble. Most of ensemble-processing strategies, however, use criteria involving a single variable (often the variable of relevant climate interest or a more-elaborated compound index), while the simulation ability of different climate models varies greatly for different variables. The lack of multiple constraints constitutes a shortcoming for this kind of practices. In the climate system, geophysical variables are physically connected to each other. A multi-objective optimization applied to multiple co-variables provides an interesting way to assess such processes relating multiple variables. In this work, we want to promote the multi-model ensemble-processing strategies that involve multiple objectives, which mimics the physically based links among variables in the climate system.

The Pareto optimality was then used to conduct multi-objective optimization, and a further scheme called Least-distance strategy was also elaborated and applied to the multi-model ensemble simulations at our disposal. The latter selected a Pareto-optimal subset with simultaneous short distance to the observation for all involved variables. The Rank-based weighting method that independently evaluates the different objectives was also used as a reference. It doesn't take into account any potential physically based links among climate variables. As an example of application, this work targets SLP of WNPSH, with SST from three physically linked oceanic basins

as co-variables. Improvements can be seen in the two multi-objective schemes in simulation of both WNPSH and SST, compared to the simple arithmetic mean across CMIP6 models. They also perform better than the Rank-based weighting method, emphasizing the importance of physical links in processing multi-model ensemble simulations.

It should be noted that all members of the Pareto-optimal subset (also called Pareto front) are not ideal states. The Pareto-optimality stipulates that “one cannot gain more benefits or interests without harming others when allocating limited resources,” which means that it faces the risk of selecting members which have poor skill (though still better than most other members in the raw ensemble) in one variable, but selected due to their better performance in another variable. This issue was not discussed in previous studies. To take it into account, we added a further constraint: the least distance from observation. This scheme shows the best performance in both SLP and SST climatology. The results confirm that there are some Pareto-optimal members with relatively poor performance and such members can be eliminated by the Least-distance strategy.

Conflict of Interest

The authors declare no conflicts of interest relevant to this study.

Data Availability Statement

The data sets used in this study are all freely available. CMIP6 model data are from the Earth System Grid Federation (<https://esgf-node.llnl.gov/search/cmip6/>), models used in this study are listed in Table S1 in Supporting Information S1. Observational SLP data is from the European Centre for Medium-Range Weather Forecasts (ECMWF) fifth-generation (ERA5) reanalysis data sets (<https://doi.org/10.24381/cds.f17050d7>). Observational SST data is from the National Oceanic and Atmospheric Administration (NOAA) Extended Reconstructed Sea Surface Temperature data set version 5 (ERSSTv5) (<https://www.ncei.noaa.gov/products/extended-reconstructed-sst>).

Acknowledgments

This research is supported by the National Natural Science Foundation of China (Grant 42275184) and the National Key Research and Development Program of China (Grant 2017YFA0603804). We would like to acknowledge the World Climate Research Programme's Working Group on Coupled Modelling, which is responsible for CMIP. We thank the climate modeling groups for producing and making their model outputs available. Laurent Li acknowledges the French GENCI for allocation of computing resources. We acknowledge ECMWF for providing the observational SLP data sets (ERA5) and NOAA for providing the observational SST data sets (ERSSTv5). We also thank Baird Langenbrunner and Neelin (2017b) for releasing the Pareto-optimal algorithm.

References

- Chen, W., Jiang, Z., & Li, L. (2011). Probabilistic projections of climate change over China under the SRES A1B scenario using 28 AOGCMs. *Journal of Climate*, 24(17), 4741–4756. <https://doi.org/10.1175/2011JCLI4102.1>
- Chen, X., Zhou, T., Wu, P., Guo, Z., & Wang, M. (2020). Emergent constraints on future projections of the western North Pacific subtropical high. *Nature Communications*, 11(1), 2802. <https://doi.org/10.1038/s41467-020-16631-9>
- Chuang, P. H., Sui, C. H., & Li, T. (2011). Interannual relationships between the tropical sea surface temperature and summertime subtropical anticyclone over the western North Pacific. *Journal of Geophysical Research*, 116(D13), D13111. <https://doi.org/10.1029/2010JD015554>
- He, C., Zhou, T., Lin, A., Wu, B., Gu, D., Li, C., & Zheng, B. (2015). Enhanced or weakened Western North Pacific subtropical high under global warming? *Scientific Reports*, 5(1), 16771. <https://doi.org/10.1038/srep16771>
- He, C., Zhou, T., & Wu, B. (2015). The key ocean regions responsible for the interannual variability of the western North Pacific subtropical high and the impacting mechanisms (in Chinese). *Journal of Meteorological Research*, 29(4), 562–575. <https://doi.org/10.1007/s13351-015-5037-3>
- Herger, N., Abramowitz, S., Sherwood, R., Knutti, R., Angéilil, O., & Sisson, S. A. (2019). Ensemble optimisation, multiple constraints and overconfidence: A case study with future Australian precipitation change. *Climate Dynamics*, 53(3–4), 1581–1596. <https://doi.org/10.1007/s00382-019-04690-8>
- Hersbach, H. B., Bell, P., Berrisford, S., Hirahara, S., Horányi, A., Muñoz-Sabater, J., et al. (2020). The ERA5 global reanalysis. *Quarterly Journal of the Royal Meteorological Society*, 146(730), 1999–2049. <https://doi.org/10.1002/qj.3803>
- Hong, C., Chang, T., & Hsu, H. (2014). Enhanced relationship between the tropical Atlantic SST and the summertime western North Pacific subtropical high after the early 1980s. *Journal of Geophysical Research: Atmosphere*, 119(7), 3715–3732. <https://doi.org/10.1002/2013JD021394>
- Huang, B. P., Thorne, V., Banzon, T., Boyer, T., Chepurin, G., Lawrimore, J. H., et al. (2017). Extended reconstructed Sea Surface temperature version 5 (ERSSTv5), upgrades, validations, and intercomparisons. *Journal of Climate*, 30(20), 8179–8205. <https://doi.org/10.1175/JCLI-D-16-0836.1>
- Huang, Y., Li, X., & Wang, H. (2016). Will the western Pacific subtropical high constantly intensify in the future? *Climate Dynamics*, 47(1–2), 567–577. <https://doi.org/10.1007/s00382-015-2856-y>
- Jiang, Z., Li, W., Xu, J., & Li, L. (2015). Extreme precipitation Indices over China in CMIP5 models. Part I: Model evaluation. *Journal of Climate*, 28(21), 8603–8619. <https://doi.org/10.1175/JCLI-D-15-0099.1>
- Langenbrunner, B., & Neelin, J. D. (2017a). Multiobjective constraints for climate model parameter choices: Pragmatic Pareto fronts in CESM1. *Journal of Advances in Modeling Earth Systems*, 9(5), 2008–2026. <https://doi.org/10.1002/2017MS000942>
- Langenbrunner, B., & Neelin, J. D. (2017b). Pareto-optimal estimates of California precipitation change. *Geophysical Research Letters*, 44(12), 12436–12446. <https://doi.org/10.1002/2017GL075226>
- Li, C., Lu, R. N., Dunstone, N., Scaife, A. A., Bett, P. E., & Zheng, F. (2021). The seasonal prediction of the exceptional Yangtze River rainfall in summer 2020. *Advances in Atmospheric Sciences*, 38(12), 2055–2066. <https://doi.org/10.1007/s00376-021-1092-0>
- Li, F., Zhu, Q., Riley, W., Yuan, K., Wu, H., & Gui, Z. (2022). Wetter California projected by CMIP6 models with observational constraints under a high GHG emission scenario. *Earth's Future*, 10(4), e2022EF002694. <https://doi.org/10.1029/2022EF002694>
- Li, T., Jiang, Z., Zhao, L., & Li, L. (2021). Multi-model ensemble projection of precipitation changes over China under global warming of 1.5 and 2°C with consideration of model performance and independence. *Journal of Meteorological Research*, 35(1), 184–197. <https://doi.org/10.1007/s13351-021-0067-5>

- Li, T., Jiang, Z. H., Treut, L., Li, L., Zhao, L., & Ge, L. (2021). Machine learning to optimize climate projection over China with multi model ensemble simulations. *Environmental Research Letters*, *16*(9), 094028. <https://doi.org/10.1088/1748-9326/ac1d0c>
- Li, W., Jiang, Z., Xu, J., & Li, L. (2016). Extreme precipitation Indices over China in CMIP5 models. Part 2 Probabilistic projection. *Journal of Climate*, *29*(24), 8989–9004. <https://doi.org/10.1175/JCLI-D-16-0377.1>
- Li, Y., Yang, X. Q., & Xie, Q. (2010). Selective interaction between interannual variability of North Pacific subtropical high and ENSO cycle. *Chinese Journal of Geophysics*, *53*(7), 1543–1553. <https://doi.org/10.3969/j.issn.0001-5733.2010.07.005>
- Luo, M., & Lau, N. C. (2017). Heat waves in southern China: Synoptic behavior, long-term change and urbanization effects. *Journal of Climate*, *30*(2), 703–720. <https://doi.org/10.1175/JCLI-D-16-0269.1>
- Pareto, V. (1906). *Manuale di economia politica* (Vol. 13). Societa Editrice.
- Preethi, B. M., Mujumdar, A., Prabhu, A., & Kripalani, R. (2017). Variability and teleconnections of South and East Asian summer monsoons in present and future projections of CMIP5 climate models. *Asia-Pacific Journal of Atmospheric Sciences*, *53*(2), 305–325. <https://doi.org/10.1007/s13143-017-0034-3>
- Song, F., & Zhou, T. (2014). Interannual variability of East Asian summer monsoon simulated by CMIP3 and CMIP5 AGCMs: Skill dependence on Indian Ocean–western Pacific anticyclone teleconnection. *Journal of Climate*, *27*(4), 1679–1697. <https://doi.org/10.1175/JCLI-D-13-00248.1>
- Tan, J., Jiang, Z., & Ma, T. (2016). Projections of future surface air temperature change and uncertainty over China based on the Bayesian Model Averaging (in Chinese). *Acta Meteorologica Sinica*, *74*(4), 583–597. <https://doi.org/10.11676/qxb2016.044>
- Taylor, K. (2001). Summarizing multiple aspects of model performance in a single diagram. *Journal of Geophysical Research*, *106*(D7), 7183–7192. <https://doi.org/10.1029/2000JD900719>
- Wang, B., Wu, R., & Fu, X. (2000). Pacific-East Asian tele-connection: How does ENSO affect East Asian climate? *Journal of Climate*, *13*(9), 1517–1536. [https://doi.org/10.1175/1520-0442\(2000\)013<1517:PEATHD>2.0.CO;2](https://doi.org/10.1175/1520-0442(2000)013<1517:PEATHD>2.0.CO;2)
- Wang, B., Xiang, B., & Lee, J. (2013). Subtropical High predictability establishes a promising way for monsoon and tropical storm predictions. *Proceedings of the National Academy of Sciences of the United States of America*, *110*(8), 2718–2722. <https://doi.org/10.1073/pnas.1214626110>
- Wang, W., Zhou, W., Li, X., Wang, X., & Wang, D. (2016). Synoptic-scale characteristics and atmospheric controls of summer heat waves in China. *Climate Dynamics*, *46*(9–10), 2923–2941. <https://doi.org/10.1007/s00382-015-2741-8>
- Woodruff, M. J., & Herman, J. D. (2014). Pareto.py: Nondominated sorting for multi-objective problems. Retrieved from <https://github.com/matthewjwoodruff/pareto.py>
- Wu, B., Zhou, T., & Li, T. (2009). Seasonally evolving dominant interannual variability modes of East Asian climate. *Journal of Climate*, *22*(11), 2992–3005. <https://doi.org/10.1175/2008JCLI2710.1>
- Xiang, B., Wang, B., Yu, W., & Xu, S. (2013). How can anomalous western North Pacific Subtropical High intensify in late summer? *Geophysical Research Letters*, *40*(10), 2349–2354. <https://doi.org/10.1002/grl.50431>
- Xie, S. J., Hafner, H., Tokinaga, H., Du, Y., Huang, G., & Sampe, T. (2009). Indian Ocean capacitor effect on Indo-Western Pacific climate during the summer following El Niño. *Journal of Climate*, *22*(3), 730–747. <https://doi.org/10.1175/2008JCLI2544.1>
- Ying, M., & Sun, S. (2000). A study on the response of subtropical high over the Western Pacific on the SST anomaly (in Chinese). *Chinese Journal of Atmospheric Sciences*, *24*(2), 193–206. <https://doi.org/10.11676/qxb2016.044>
- Zeng, G., Sun, Z., Lin, Z., & Ni, D. (2010). Numerical simulation of impacts of sea surface temperature anomaly upon the interdecadal variation in the northwestern Pacific subtropical high (in Chinese). *Chinese Journal of Atmospheric Sciences*, *34*(2), 307–322. <https://doi.org/10.3878/j.issn.1006-9895.2010.02.06>
- Zhang, Q., & Tao, S. (2003). The anomalous subtropical anticyclone in western Pacific and their association with circulation over East Asia during summer (in Chinese). *Chinese Journal of Atmospheric Sciences*, *3*, 369–380. <https://doi.org/10.3878/j.issn.1006-9895.2003.03.07>
- Zhao, C., Jiang, Z., Sun, X., Li, W., & Li, L. (2020). How well do climate models simulate regional atmospheric circulation over East Asia? *International Journal of Climatology*, *40*(1), 220–234. <https://doi.org/10.1002/joc.6205>
- Zhou, T., Wu, B., Guo, Z., He, C., Zou, L., Chen, X., et al. (2018). A review of East Asian summer monsoon simulation and projection: Achievements and problems, opportunities and challenges (in Chinese). *Chinese Journal of Atmospheric Sciences*, *42*(4), 902–934. <https://doi.org/10.3878/j.issn.1006-9895.1802.17306>
- Zhou, T., Yu, R., Zhang, J. H., Drange, H., Cassou, C., Deser, C., et al. (2009). Why the western Pacific subtropical high has extended westward since the late 1970s. *Journal of Climate*, *22*(8), 2199–2215. <https://doi.org/10.1175/2008JCLI2527.1>
- Zhu, H., Jiang, Z., Li, J., Li, W., Sun, C., & Li, L. (2020). Does CMIP6 inspire more confidence in simulating climate extremes over China? *Advances in Atmospheric Sciences*, *37*(10), 1119–1132. <https://doi.org/10.1007/s00376-020-9289-1>
- Zhu, J., Yu, Y., Guan, Z., & Wang, X. (2022). Dominant coupling mode of SST in Maritime continental region and East Asian summer monsoon circulation. *Journal of Geophysical Research: Atmospheres*, *127*(19), e2022JD036739. <https://doi.org/10.1029/2022JD036739>
- Zuo, J. W., Li, C., Sun, C., & Ren, H. C. (2019). Remote forcing of the northern tropical Atlantic SST anomalies on the western North Pacific anomalous anticyclone. *Climate Dynamics*, *52*(5–6), 2837–2853. <https://doi.org/10.1007/s00382-018-4298-9>